Transcriptional variability accelerates pre-leukemia by cell diversification and perturbation of protein synthesis

Short title: **Loss of Kat2a accelerates pre-leukemia**

One-sentence summary: **Loss of Kat2a enhances transcriptional variability of ribosome biosynthetic programs and transiently accelerates pre-leukemia**

Shikha Gupta[1,2], Oliver M. Dovey[3#], Ana Filipa Domingues[2,4], Oliwia W. Cyran[2], Caitlin M. Cash[5], George Giotopoulos[2,4], Justyna Rak[2,4], Jonathan Cooper[2,3,4], Malgorzata Gozdecka[2,4], Ryan J. Asby[2,4], Noor Al-Jabery[5], Victor Hernandez-Hernandez[5,6], Sudhakaran Prabakaran[1,7¶], Brian J. Huntly[2,4], George S. Vassiliou[2,3,4], Cristina Pina[5,6*]

[1]Department of Genetics, University of Cambridge, UK; [2]Department of Haematology, University of Cambridge, UK; [3]Wellcome Sanger Institute, Wellcome Trust Genome Campus, UK; [4]Wellcome Trust-MRC Cambridge Stem Cell Institute, University of Cambridge, UK; [5]College of Health, Medicine and Life Sciences - Division of Biosciences, Brunel University London, UK; [6]Centre for Genome Engineering and Maintenance, Brunel University London, Uxbridge, UB8 3PH, UK; [7]NonExomics, Inc., USA *corresponding author (cristina.pina@brunel.ac.uk)

[#]Current address: Bit.Bio; Babraham Research Campus; Cambridge, CB22 3FH; UK

[¶]Current address: NonExomics, Inc., 2 Simon Willard Rd, Acton, MA 01720, USA

Abstract: **Transcriptional variability facilitates stochastic cell diversification and can in turn underpin adaptation to stress or injury. We hypothesize that it may analogously facilitate progression of pre-malignancy to cancer. To investigate this, we initiated pre-leukemia in mouse cells with enhanced transcriptional variability due to conditional disruption of the histone lysine acetyltransferase gene *Kat2a*. By combining single-cell RNA-sequencing of pre-leukemia with functional analysis of transformation, we show that *Kat2a* loss results in global variegation of cell identity and accumulation of pre-leukemic cells. Leukemia progression is subsequently facilitated by destabilization of ribosome biogenesis and protein synthesis, which confer a transient transformation advantage. The contribution of transcriptional variability to early cancer evolution**

reflects a generic role in promoting cell fate transitions, which, in the case of well-adapted malignancies, contrastingly differentiates and depletes cancer stem cells. In other words, transcriptional variability confers forward momentum to cell fate systems, with differential multi-stage impact throughout cancer evolution.

Tumors evolve by genetic drift and natural selection [1,2]. Acquisition of new mutations confers a probability of adaptation to new environmental pressures [3], and facilitates progression and transformation of pre-malignant lesions, promotes metastasis and drives treatment resistance [4]. In recent years, it became apparent that non-genetic instability, in particular variability in methylation epialleles, can confer adaptive advantages to tumor growth and survival irrespective of mutations, and function as drivers of therapy resistance and disease relapse in hematological malignancies [5,6]. Hematological malignancies, and in particular Acute Myeloid Leukemia (AML), are strongly dependent on epigenetic regulation, both through mutation of chromatin factors, and by co-option of unmutated chromatin regulators into maintenance of leukemogenic programs [7–9]. Notably, AML has lower levels of mutations than solid tumors, supporting the notion that non-genetic events may be especially important in the former [7]. Akin to genetic instability, epigenetic variability is increased in leukemia initiation and relapse, but low in leukemia maintenance [10,11], suggesting that reconfiguration of molecular/transcriptional programs may perturb the identity or survival of well-adapted leukemia cells by disrupting pro-oncogenic molecular signatures. We have recently captured this phenomenon upon loss of KAT2A, a histone acetyltransferase that promotes gene transcription through activation of promoter bursting and stabilization of gene expression levels. *Kat2a* loss (NULL) results in enhanced cell-to-cell transcriptional variability and progressive loss of leukemia stem cells (LSC) transformed with the *KMT2A-MLLT3* (*MLL-AF9*) gene fusion [12]. Accordingly, KAT2A is required for maintenance of AML cell lines and *in vitro* self-renewal of patient AML blasts [13]. At a cellular level, loss of *Kat2a* results in perturbation of leukemia lineage trajectories, with emergence of multiple incongruent differentiation pathways that deplete LSC, but fail to uniformly differentiate leukemia cells [12]. A similar pattern of incongruous exit from the stem cell state was observed upon KAT2A inhibition in mouse embryonic stem (ES) cells [14]. MLL-AF9 results in an aggressive leukemia, both in mice and in humans, and requires minimal cooperativity from additional mutational events [7,15]. As such, it provides a good representation of a well-adapted leukemia, with minimal genetic and epigenetic variability. However, it does not reflect what is observed with more common forms of AML such as those associated with *RUNX1-*

69 *RUNX1T1* (*AML1-ETO*), where progression in mouse models is slow and infrequent [7,16], or
70 clonal hematopoiesis, in which the associated mutations (e.g. in *IDH1/2*, *TET2*, *DNMT3A*)
71 convey a self-renewal advantage, but require additional genetic events for leukemia [7,16]. In
72 these cases, we postulate that malignant progression may be facilitated by non-genetic
73 instability, which can be promoted through loss of *Kat2a*.
74
75 To test our hypothesis, we made use of 2 pre-leukemia mouse models: *Idh1*^{R132H} and *RUNX1-*
76 *RUNX1T1(RT1(9a))*. First, we developed a new inducible *Idh1*^{R132H} allele (Fig. S1a-c, and
77 Supplementary Methods), and crossed it into an *Mx1-Cre* background (Fig. S1d), to activate
78 the mutation in hematopoietic tissues. We verified the functionality of the *Idh1*^{R132H} allele by
79 accumulation of the onco-metabolite 2-HG (Fig. S1e-f). *Idh1*^{R132H} mice develop
80 leukemia rarely, with long latency and low penetrance, with no significant effects on overall
81 survival (Fig. S1g). In contrast, combination of *Idh1*^{R132H} with other leukemogenic
82 mutations, namely *NRas* and *Npm1c* (triple-mutant), results in short-latency high-penetrance
83 leukemia development (Fig. S1g), confirming the pre-leukemic nature of the *Idh1*^{R132H}
84 model. Accordingly, triple-mutant BM cells, but not cells with *Idh1*^{R132H} alone, have enhanced
85 colony-forming cell (CFC) assay replating ability, an *in vitro* measure of
86 transformation (Fig. S1h). Comparison of RNA-sequencing from triple-mutant leukemias vs
87 triple-mutant pre-leukemias, or vs *Idh1*^{R132H} alone, revealed a gene signature which was
88 specific to the leukemia state, and in which down-regulated genes were enriched
89 for *Kat2a* chromatin targets (Fig. S1i). This association suggests that loss of Kat2a activity
90 may contribute to progression of pre-leukemia to overt AML.
91
92 To investigate this putative contribution of *Kat2a* loss to pre-leukemia progression, we
93 crossed conditional *Idh1*^{R132H} and *Kat2a*$^{Flox/Flox}$ mice, into the Mx1-Cre background (Fig.1a), to
94 generate *Idh1*^{R132H} animals that were heterozygous (HET) or NULL for *Kat2a* (Fig. S2a-
95 b). We analyzed *Idh1*^{R132H} *Kat2a*$^{Flox/WT}$ (*Idh*^{mut} *Kat2aHET*) and
96 *Idh1*^{R132H} *Kat2a*$^{Flox/Flox}$ (*Idh*^{mut}*Kat2aNULL*) animals 4 and 20 weeks after Cre induction, to
97 identify early and progressed *Idh1*^{R132H} pre-leukemia states. Analysis of BM stem and
98 progenitor composition revealed no differences between genotypes or timepoints (Fig.S2c-
99 g). We did not observe differences in spleen or liver pre-leukemia burden (Fig.S2h-
100 i). However, *Idh*^{mut} *Kat2aNULL* samples had a significant advantage in CFC re-plating in
101 early pre-leukemia (4 weeks) (Fig.1b), which was not sustained at the 20-week timepoint.

Fig 1

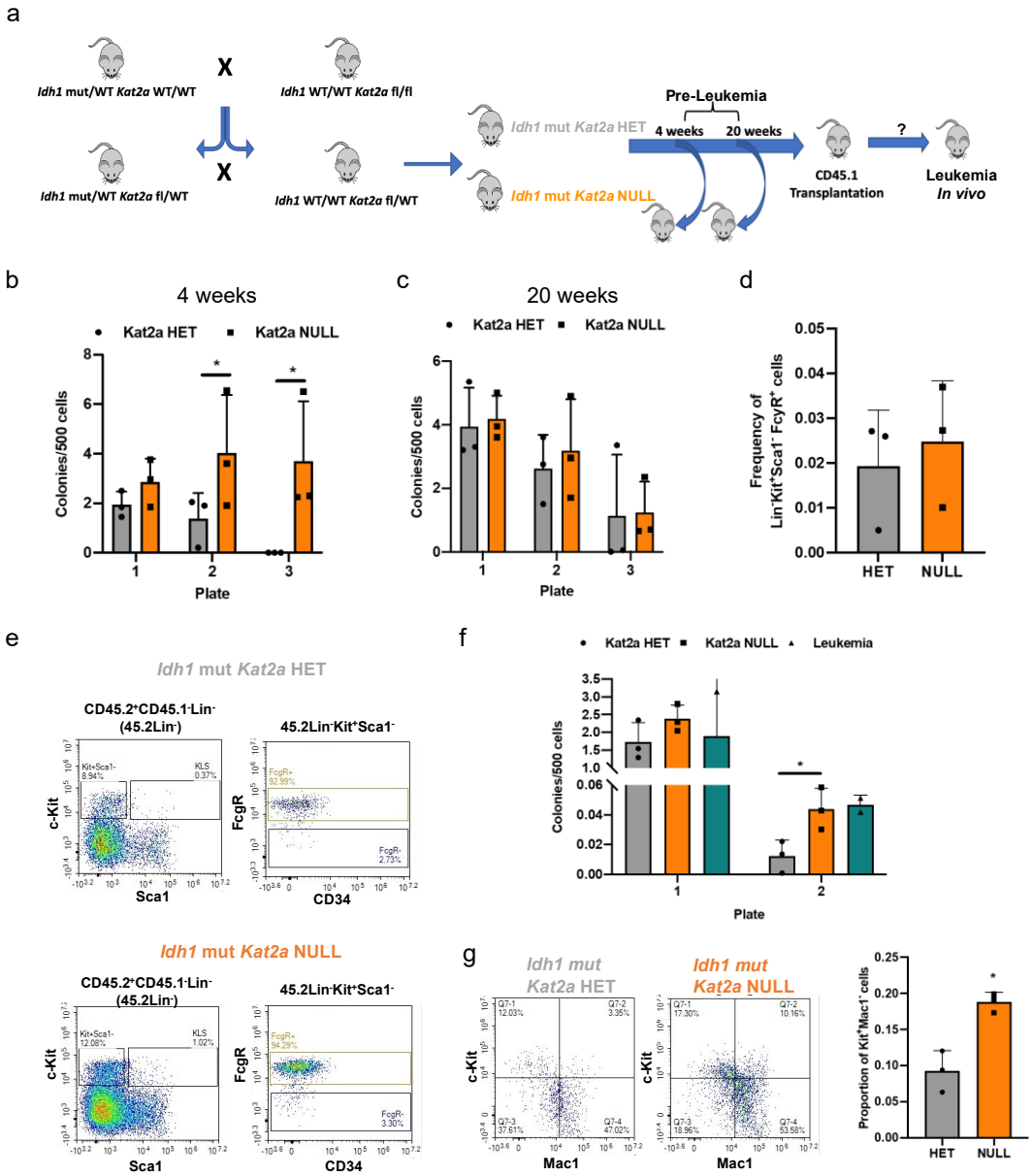

Fig. 1: *Kat2a* loss facilitates development of *Idh1*^{R132H} pre-leukemia. (A) Diagram of *Idh1*^{R132H} (*Idh1* mut) and *Kat2a* $^{fl/fl}$ mouse crosses to generate *Idh1* mut *Kat2a* HET and *Idh1* mut *Kat2a* NULL cells used in pre-leukemia studies. **(B)** Colony-forming cell (CFC) assays of *Idh1* mut *Kat2a* HET and NULL BM cells 4 weeks post-pIpC treatment; mean ± SD, n=3. **(C)** Colony-forming cell (CFC) assays of *Idh1* mut *Kat2a* HET and NULL BM cells 20 weeks post-pIpC treatment; mean ± SD, n=3. **(D)** Quantification of GMP-like BM cells obtained from *Idh1* mut CD45.2^{+} grafts; mean ± SD, n=3 irradiated recipients (CD45.1). **(E)** Representative flow cytometry plots of BM cells in (D); top: *Idh1* mut *Kat2a* HET, bottom: *Idh1* mut *Kat2a* NULL. **(F)** Serial re-plating CFC assays of *Idh1* mut BM grafts. Mean ± SD, n=3 *Idh1* mut *Kat2a* HET and NULL, n=2 *Idh1* mut leukemia. **(G)** Flow cytometry of colonies in (F), Left, representative plots; right, Kit^{+} Mac1^{-} progenitor quantification. Mean ± SD, n=3. All analyses 2-tailed t-test; significant *p<0.05.

114 This could be compatible with earlier selection of pre-leukemia cells upon *Kat2a* loss, which
115 is achieved later in *Idh*^{mut} *Kat2aHET* animals as the *Idh1*^{mut} phenotype progresses (Fig. 1c).
116 In an attempt to understand whether the early replating advantage *in vitro* could lead to
117 accelerated leukemia development *in vivo* in the absence of other genetic events, we
118 transplanted BM cells from *Idh*^{mut} *Kat2aHET* and *Idh*^{mut} *Kat2aNULL* mice, into irradiated
119 CD45.1 recipients and followed them up for 1 year. Similar to single *Idh1*^{mut} animals, we
120 could not detect signs of leukemia development in transplanted mice (Fig. S3a). Transplants
121 showed accumulation of GMP-like (Lin-Kit^{+}Sca1^{-}FcγR^{+}) donor cells, compatible
122 with myeloproliferation (Fig. 1d-e), which was identical between genotypes. Peripheral blood
123 counts (Fig.S3b-d) and spleen and liver weights (Fig.S3e-f) were also similar. However, we
124 observed infiltration of spleen and liver in 1 of 3 *Idh*^{mut} *Kat2aNULL* recipients, which was
125 not present in *Idh*^{mut} *Kat2aHET* grafts (Fig.S3g). Notably, *Idh*^{mut} *Kat2aNULL* cells showed
126 enhanced colony-replating potential relative to *Idh*^{mut} *Kat2aHET*, which was comparable to
127 that of BM from rare *Idh*^{mut} leukemic animals (Fig. 1f). *Idh*^{mut} *Kat2aNULL* cells in CFC
128 assays were enriched in c-Kit^{+}Mac1^{-} cells (Fig. 1g) compatible with hindered differentiation
129 and/or expansion of self-renewing cells. Overall, the results suggest that loss
130 of *Kat2a* imparts leukemogenic properties to *Idh1*^{mut} cells but is in itself not sufficient to
131 drive leukemogenesis in the absence of additional cooperating genetic events.
132
133 We next tested the impact of *Kat2a* loss on the pre-leukemia model driven by the exon 9a
134 splicing variant of the *RUNX1-RUNX1T1* (*RT1(9a)*) fusion gene, which when retrovirally-
135 delivered to adult BM cells, leads to long-latency, incomplete-penetrance leukemia in
136 irradiated recipients. Using our previously described *Kat2a*$^{Flox/Flox}$ *Mx1-Cre* mice, we
137 isolated progenitor-enriched BM cells after *pIpC*-induced locus excision (Fig. S4a),
138 and delivered the RT1(9a) construct by retroviral transduction, as described [17]. In all
139 experiments, *Kat2a*$^{Flox/Flox}$ *Mx1-Cre*$^{+/-}$ (*Kat2aNULL*) were compared with *Kat2a*$^{Flox/Flox}$ *Mx1-*
140 *Cre*$^{-/-}$ (*Kat2aWT*) cells. We started by evaluating leukemia development after
141 transplantation of RT1(9a) *Kat2aNULL* and *Kat2aWT* BM cells (Fig. 2a). Loss of *Kat2a* led
142 to a dramatic decrease in survival of RT1(9a) recipient animals, compatible with accelerated
143 leukemia progression (Fig. 2b). *Kat2a NULL* leukemias had a non-significant trend towards
144 higher white blood cell counts (Fig. S4b-d) and spleen leukemia burden, with
145 minimal infiltration of other organs (Fig. S4e-g). The surface phenotype of the
146 leukemias was indistinguishable between genotypes (Fig. S4h). Analysis of early timepoints
147 post-transplantation showed that RT1(9a) engraftment became quickly fixed in the absence

Fig 2

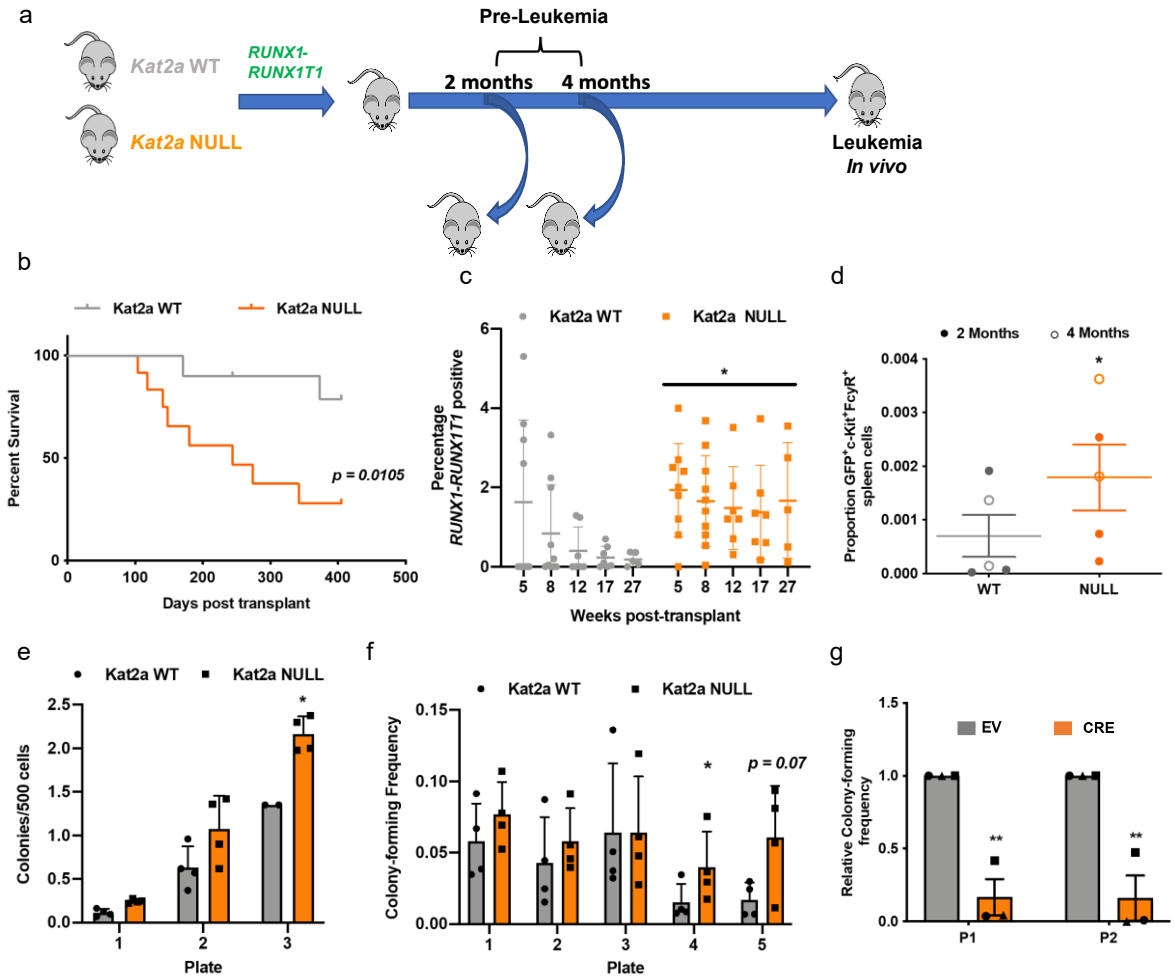

148

149 **Fig. 2: *Kat2a* loss accelerates *RT1(9a)* pre-leukemia to leukemia progression. (A)** Experimental design. **(B)**
150 Survival curve of *RT1(9a) Kat2aWT* and *Kat2aNULL* Kit^{+} BM recipients; n=12 animals/genotype, *p<0.05, log-rank
151 test. **(C)** Quantification of peripheral blood GFP for animals in (A); GFP reports *RT1(9a)*. Mean ± SD, n=10
152 animals/genotype (8 weeks), *p<0.05, 2-way ANOVA. **(D)** CFC assay of *RT1(9a) Kat2aWT* and *Kat2aNULL* graft
153 BM cells 4 months post-transplantation; mean ± SD, n=4. **(E)** Flow cytometry analysis of *RT1(9a) Kat2aWT* and
154 *Kat2aNULL* graft spleen cells 2- and 4-months post-transplantation; mean ± SD, n=5. **(F)** *In vitro* transformation of
155 *Kat2aWT* and *Kat2aNULL* Lin^{-}/Kit^{+} BM cells transduced with *RT1(9a)* retrovirus tested in CFC serial re-plating;
156 mean ± SD, n=4. **(G)** CFC re-plating (plate=P1, P2) analysis of *RT1(9a) Kat2a$^{Flox/Flox}$* Cre$^{-/-}$ Kit^{+}/Lin^{-} BM cells excised
157 *in vitro* by lentiviral-delivered *Cre* recombinase (vs. EV, empty vector) after 3 rounds of colony re-plating. Mean ±
158 SD, n=3. All other analyses 2-tailed t-test, *p<0.05, **p<0.01.

159

160

161 of *Kat2a* (Fig. 2c). *Kat2aNULL/RT1(9a)* cells obtained from healthy pre-
162 symptomatic recipients were enriched for GMP-like cells (Fig. 2d), and displayed enhanced
163 colony formation (Fig. 2e), compatible with accelerated pre-leukemia

development. Similarly, *Kat2aNULL* cells directly tested in CFC assays upon retroviral transduction, displayed enhanced re-plating potential. (Fig. 2f). In contrast, excision of *Kat2a* in RT1(9a) cells post-*in vitro* transformation by 3 rounds of serial-replating, led to a reduction in colony formation (Fig. 2g), suggesting that *Kat2a* loss favors leukemia development only at a pre-leukemia stage. These observations mirror our previously identified role for *Kat2a* in maintenance of established leukemia stem-like cells and suggest that *Kat2a* plays stage-specific roles during leukemogenesis, which are preserved across leukemia models.

We had previously associated *Kat2a* function in leukemia stem cell maintenance with stability of transcriptional programs [12]. Using single-cell RNA-sequencing (scRNA-seq), we showed that *Kat2a* loss resulted in diversification and branching of differentiation trajectories, and associated with enhanced transcriptional noise, particularly in biosynthetic programs (e.g., ribosomal biogenesis and translation). We asked if similar mechanisms were at play in pre-leukemia progression facilitated by *Kat2a* loss. We hypothesized that enhanced transcriptional variability leading to program diversification might increase the probability of accessing or seeding leukemia programs, resulting in the observed acceleration in leukemia progression. We performed scRNA-seq analysis of pre-leukemia cells on the 10X platform, comparing transcriptional landscapes of *Kat2a*NULL and *Kat2a*WT RT1(9a) asymptomatic animals obtained 2 and 4 month post-transplantation. We sequenced a total of 1767 cells sorted as RT1(9a)/GFP^{+} Kit^{+} stem/progenitor and retrieved an average of 174770 aligned reads per cell, corresponding to medians of 5939 Unique Molecular Identifiers (UMI) and 1575 genes per cell (Supplementary File 1). Less than 0.2% of reads aligned to mitochondrial DNA, denoting successful sequencing. Pre-processing steps are detailed in Supplementary Methods.

We employed transcripts of cell surface markers routinely used for hematopoietic cell immunophenotyping to map the identity of cells along the pseudo-temporal trajectories (Fig. S5a-b). Cells at the origin of the trajectory expressed high *Ly6e* (*Sca1*), *Cd34* and *Flt3*, compatible with lymphoid-myeloid-primed progenitors (LMPP). LMPPs were adjacent to a granulocyte-monocyte progenitor (GMP)-like state (*Ly6e*^{low}*Cd34*$^{+}$*Fcgr3*$^{+}$). Trajectories involved 3 additional states: *Ly6e*$^{+}$ *CD79a*$^{+}$ *Cd14*$^{-}$ B-cell affiliated Progenitor (BAP) (Supplementary File 3), and *Ly6e*$^{+}$*Fcgr3*$^{+}$*Cd14*$^{+}$ Monocyte-affiliated Progenitor (MAP)

Fig 3

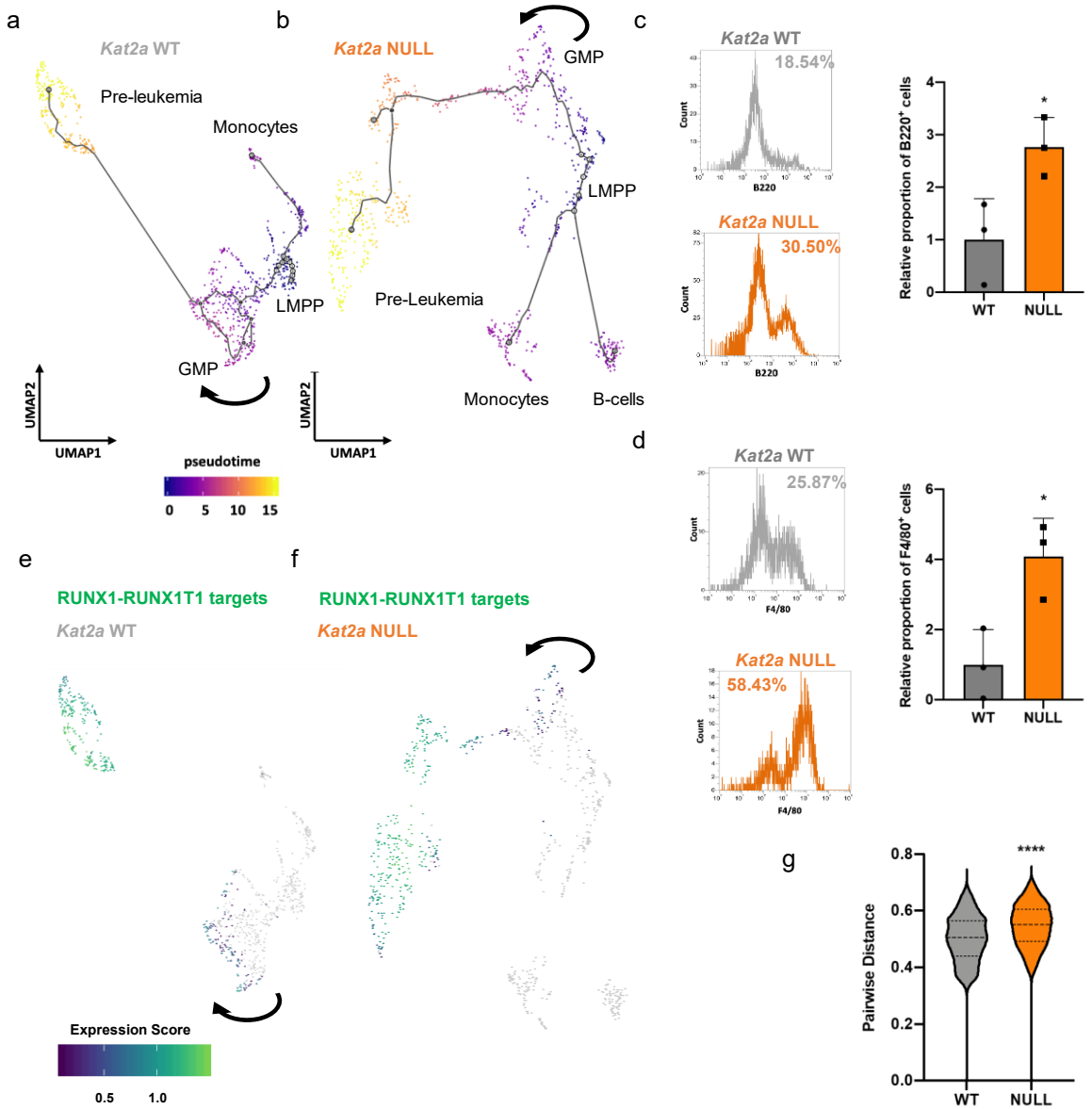

Fig. 3: Loss of *Kat2a* diversifies cell fates and promotes RT1(9a) pre-leukemia progression. (A-B) Pseudotime single-cell trajectory of **(A)** *Kat2aWT* cells, **(B)** *Kat2aNULL* RT1(9a) cells 2 and 4 months after transplantation. Trajectories inferred using Monocle3 [21]; compartments labelled as per hematopoietic markers in Fig. S5A- B. Arrows denote pseudotime progression. **(C)** B220 B-cell marker in plate 2 CFC of RT1(9a)-transduced *Kat2aWT* and *Kat2aNULL* cells during *in vitro* transformation; mean ± SD, n=3. **(D)** F4/80 monocyte marker in plate 2 CFC of RT1(9a)-transduced *Kat2aWT* and *Kat2aNULL* cells during *in vitro* transformation; mean ± SD, n=3. **(E-F)** Expression of *RUNX1-RUNX1T1* ChIP-seq targets [18] in **(E)** *Kat2aWT* cells and **(F)** *Kat2aNULL* RT1(9a) single-cell trajectories. Arrows as in A-B. **(G)** Pairwise distance transcriptional variability measure[19] of *Kat2aWT* and *Kat2aNULL* RT1(9a) cells; top 500 most variable genes/genotype calculated by distance to the median CV (DM); ****p-adj<0.0001. All analyses 2-tailed t-test, *p<0.05.

210 (Supplementary File 4), confirmed by gene ontology (GO) analysis (Fig. S5c-d); and a third
211 compartment in direct proximity of the GMP, characterized as *Ly6e*$^{+}$*Fcgr3*$^{+}$*Cd33*$^{+}$*Cd14*$^{+}$,
212 with no*Cd34* or *Cd48*. BAP was exclusive to *Kat2a*NULL samples, while MAP was
213 common to both genotypes, albeit enriched in *Kat2a*NULL samples (Fig. S5e). We
214 confirmed enhanced phenotypic differentiation of *Kat2a*NULL RT1(9a) cells to the B (Fig.
215 3c) and macrophage (Fig. 3d) lineages *in vitro*. Using a signature of RT1 chromatin targets [18],
216 we identified the third compartment as the candidate pre-leukemia progenitor (PLP)
217 population (Fig. 3e-f). PLPs form a discrete (Fig. 3e) and relatively smaller
218 (Fig. S5e) compartment in the *Kat2a*WT trajectory; in contrast, the GMP-to-PLP transition
219 is more densely populated in *Kat2a*NULL pre-leukemia (Fig. 3f), with PLP comprising a
220 larger number of NULL cells. (Fig. S5e). Overall, the pseudo-temporal trajectories support
221 the notion of increased cell diversification through *Kat2a* loss, with additional cell states
222 (BAP) and, importantly, increased size of the PLP compartment. Comparative analyses of 2
223 and 4-month pre-leukemia samples confirm the pseudo-temporal trajectory
224 findings: *Kat2a*WT RT1(9a) cells progressively differentiate from LMPP to GMP-like
225 cells (Fig. S5f) and accumulate PLPs. Pre-leukemia progression is accelerated
226 in *Kat2a*NULL RT1(9a) (Fig. S5f), which contain nearly 50% of PLPs at 4 months,
227 and uniquely display 27% of BAP cells at 2 months (Fig. S5f). The increased diversification
228 of cell types in *Kat2a* NULL samples translated in enhanced cell-to-cell transcriptional
229 variability, measured by pairwise distance [19] (Fig. 3g, S6a). *Kat2a*NULL transcriptional
230 programs were also more variable within individual cell sub-populations (Fig. S6b),
231 indicating that the variability is likely to at least in part reflect transcriptional noise, rather
232 than differences in cellular composition alone. Comparison of transcriptional
233 variability between *Kat2a* WT and NULL cell subpopulations shows that the GMP to PLP
234 transition itself is accompanied by enhanced transcriptional variability (Fig. S6b), supporting
235 the notion that *Kat2a* loss may accelerate pre-leukemia progression through enhanced
236 transcriptional noise.
237
238 In order to understand the nature of the transcriptional programs perturbed upon (1) *Kat2a*
239 loss, and (2) pre-leukemia progression, we performed differential gene expression analysis of
240 the scRNA-seq dataset. Comparison of *Kat2a*NULL to WT cells revealed minimal changes in
241 gene expression levels (Fig. S7a), which were of down-regulation, as previously observed
242 upon *Kat2a* loss [12]. Consistent with our published data [12], differentially-expressed genes
243 between genotypes predominantly associated with ribosomal assembly and translation

Fig 4

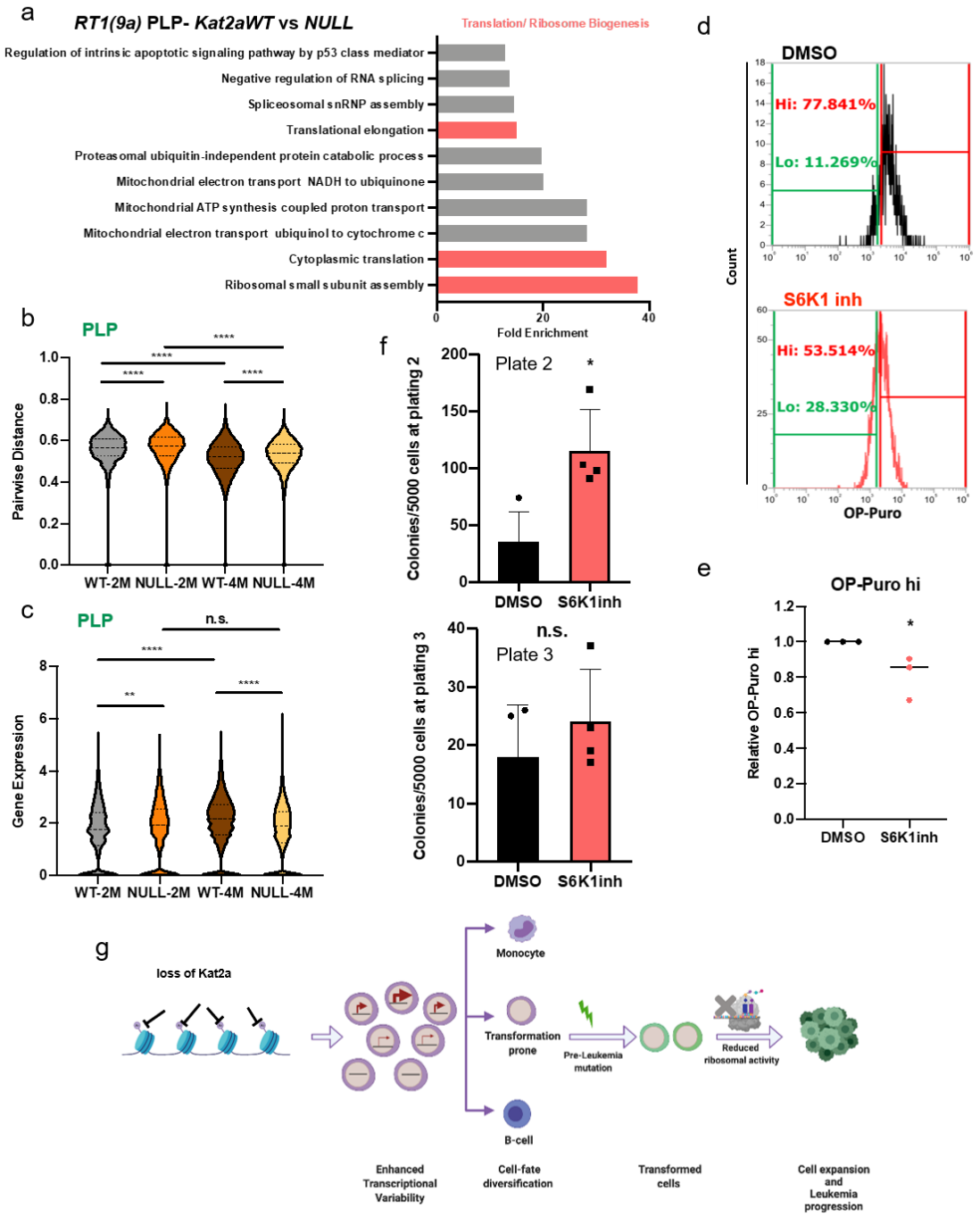

Fig. 4: Inhibition of protein synthesis phenocopies effects of *Kat2a* loss facilitating pre-leukemia transformation. (A) Over-represented gene ontology categories (GO) for genes downregulated in RT1(9a) *Kat2aNULL* vs. *WT* PLP; *p-adj<0.05. **(B)** Pairwise distance [19] of RT1(9a) PLPs; comparisons consider correlations between ribosomal biogenesis genes ****p-adj<0.0001, 2-tailed t-test. **(C)** Distribution of expression levels for gene signatures in (B) ****p-adj<0.0001, 2-tailed t-test. **(D)** Representative OP-Puro incorporation flow cytometry of S6K1inh-treated RT1(9a) *Kat2aWT* cells. **(E)** Quantification of OP-Puro high cells in (E), relative to DMSO; mean ± SD, n=3, *p<0.05, 2-tailed t-test. **(F)** CFC replating of *Kat2aWT* RT1(9a) *in vitro* transformation in the presence of S6K1inh (control, DMSO). Plate 2 (left); mean ± SD, n=4, *p<0.05. Plate 3 (right); mean ± SD, n=4, n.s; 2-tailed t-test. **(G)** Proposed mode of action of *Kat2a* loss in pre-leukemia progression.

254 ontologies (Fig. S7b) (Supplementary File 5), a pattern particularly prominent within
255 PLP (Fig. 4a) (Supplementary File 6). The same ontologies were specifically down-
256 regulated in *Kat2a*WT RT1(9a) PLPs compared to other cell states (Fig. S7c) (Supplementary
257 File 7), capturing a reported decrease in protein synthesis in RT1 leukemia [20]. Ribosomal and
258 translation ontologies (Fig. S7d-e) (Supplementary File 8) were also down-regulated
259 in *Idh1*^{R132H} mice upon pre-leukemia-to-AML progression through additional genetic
260 mutations. Altogether, our findings suggest a specific association of attenuated ribosomal
261 programs with pre-leukemia progression, which may be further facilitated
262 by *Kat2a* loss. *Kat2a* loss increases variability of ribosomal biogenesis programs in PLPs
263 (Fig. 4b), themselves more variable than GMPs (Fig. S7f), suggesting enhanced noise at the
264 transition (Supplementary File 9). The gene expression range in *Kat2a*NULL PLPs favors
265 lower mean values (Fig. 4c). In support of the functional impact of the transcriptional
266 perturbation, *Kat2a* loss results in decreased protein synthesis (Fig. S8a-b; also [12]).
267
268 We tested the contribution of reduced protein synthesis activity to pre-leukemia progression
269 by treatment with the S6K1 inhibitor (S6K1inh) PF4708671 (Fig. S8c), which impairs
270 protein synthesis activity confirmed by reduced OP-Puro incorporation in nascent peptide
271 chains (Fig. 4d-e). We treated *Kat2a*WT RT1(9a) cells with S6K1inh and tested their
272 leukemia transformation potential *in vitro* through CFC assay re-plating. S6K1-inhibited
273 cells displayed enhanced colony-formation upon re-plating (Fig. 4f), suggesting a
274 contribution to leukemia transformation. However, the increase in colony formation was
275 transient and eventually lost upon subsequent re-plating (Fig. 4f). This suggests
276 that the effects of reduced protein synthesis on leukemia cells may vary with progression of
277 transformation, reconciling our data with prior analysis of established *MLL-AF9* cells, in
278 which reduced OP-Puro incorporation associated with *Kat2a*NULL-mediated extinction of
279 leukemia stem cells [12]. We observed a similar pattern of transient increase in colony
280 formation of *Idh1*^{R132H} pre-leukemia cells treated with S6K1inh (Fig. S8d). Altogether, the
281 data suggest that reduced ribosomal assembly and protein synthesis facilitate pre-leukemia
282 progression. Exploration of lower levels of expression of translation-associated genes as a
283 consequence of enhanced transcriptional variability may be instrumental in the acceleration
284 of pre-leukemia to AML transition upon *Kat2a* loss. As leukemia progresses, variability in
285 ribosomal biosynthesis programs, may become attenuated with deviation from an optimal
286 level no longer favorable to transformation.
287

288 In this report, we have shown that *Kat2a* loss facilitates pre-leukemia progression
289 in *Idh1*^{R132H} and *RUNX1-RUNX1T1(9a)* mouse models of human disease, with acceleration of
290 frank leukemia onset in the case of RT1(9a). Loss of *Kat2a* resulted in enhanced variability
291 of transcription, leading to diversification of cell fates, including accumulation of pre-
292 leukemia progenitor cells. In the context of an early genetic event such
293 as *RT1(9a)* or *Idh1*^{R132H}, which do not allow for full leukemia transformation, the cellular
294 heterogeneity that ensues creates the opportunity for specification and expansion of
295 transformation-prone cells, on which additional molecular events may act to progress the
296 leukemic process (Fig. 4g). Amongst these, we show that destabilization of translation, which
297 is specifically targeted by *Kat2a*, acts to facilitate transformation. This may be achieved by
298 surveying and selection of biosynthetically quiescent cell states, which evade further
299 diversification and respond to additional mutations with disease propagation and progression.
300 Fully transformed, well-adapted leukemia cells may buffer transcriptional variability to
301 maintain stable self-renewal signatures and optimal biosynthetic, translation rates. In this
302 context, instability of transcriptional programs may shift biosynthetic homeostasis and
303 perturb cellular identity, and mal-adapt leukemia stem-like cells, with anti-leukemia effects.
304 Thus, stage-specific tuning and untuning of transcription and translation may be employed to
305 modulate cancer progression, a principle that can be extended to other cancer state transitions
306 such as metastasis or drug-resistance with prognostic and therapeutic potential.
307
308 **ACKNOWLEDGEMENTS:**
309 **FUNDING**: This study was funded by a Lady Tata Memorial Trust International PhD
310 Scholarship to SG (2017-2021), a Kay Kendall Leukaemia Fund Intermediate Fellowship to
311 CP (KKL888), and Cancer Research UK (C22324/A23015) and Wellcome Trust
312 (WT098051) Senior Fellowships to GSV. CP was funded by a Leuka John Goldman
313 Fellowship for Future Science (2017-2019), a Wellcome Trust / University of Cambridge
314 ISSF Grant (2019) and a Start-up Grant from Brunel University London CHMLS (2019-
315 2021). Work in GSV lab is also funded by the European Research Council, Kay Kendall
316 Leukaemia Fund, Blood Cancer UK, and the Wellcome Trust. SG received partial PhD
317 studentships from the Trinity Henry Barlow and the Cambridge Commonwealth, European
318 and International Trusts, and additional support from Murray Edwards College and the
319 University of Cambridge Lundgren Award.
320 **AUTHOR CONTRIBUTIONS:** Study conception – CP; Experimental design – SG, OD,
321 GSV, CP; Data collection – SG, OD, AFD, OC, CC, GG, JR, JC, MG, RJA, NA, VH-H;

322 Data analysis and interpretation – SG, OD, AFD, OC, CC, GSV, CP; Critical reagents – SP,
323 BJH; Writing – SG, CP, with contributions from OD, GSV. All Authors approved the final
324 version of the manuscript.
325 The Authors would like to thank: Central Biomedical Services of the University of
326 Cambridge for expert animal husbandry, CRUK Genomics Core Facility at the Cambridge
327 Research Institute, and the Wellcome Trust Sanger Research Institute Genomics Core
328 Facility for library preparation and next-generation sequencing; the Flow Cytometry facilities
329 at the Cambridge Institute for Medical Research, the NIHR Cambridge BRC Cell
330 Phenotyping Hub, and the Department of Pathology of the University of Cambridge (Dr
331 Joana Cerveira) for cell sorting; Dr Roberto Bandiera for helpful discussions and reagent
332 sharing; and Dr Matt Wayland for assistance with Cell Ranger installation and 10X
333 Genomics data matrix generation.
334 **COMPETING INTERESTS:** VH-H is co-Founder and CSO of Axovia Therapeutics. SP is
335 the CEO of NonExomics, Inc. Axovia and NonExomics did not provide funding to this study,
336 and did not influence study design, execution, data analysis or interpretation.
337 **DATA AVAILABILITY:** Single-cell RNA sequencing and bulk RNA-sequencing data were
338 deposited in ArrayExpress with accession number E-MTAB-10853 and ERP006862
339 respectively.
340
341 **SUPPLEMENTARY MATERIALS**
342 Materials and Methods
343 Table S1-S3
344 Fig S1-S8
345 References 26-32
346 Supplementary Files S1-S9
347
348 **REFERENCES**
349 1. Greaves M, Maley CC. Clonal evolution in cancer. *Nature*. 2012;481(7381):306-313.
350 doi:10.1038/nature10762
351 2. N M, C S. Biological and therapeutic impact of intratumor heterogeneity in cancer
352 evolution. *Cancer Cell*. 2015;27(1):15-26. doi:10.1016/J.CCELL.2014.12.001
353 3. Zahir N, Sun R, Gallahan D, Gatenby RA, Curtis C. Characterizing the ecological and
354 evolutionary dynamics of cancer. *Nat Genet 2020 528*. 2020;52(8):759-767.
355 doi:10.1038/s41588-020-0668-4

356 4. Persi E, Wolf YI, Horn D, et al. Mutation–selection balance and compensatory
357 mechanisms in tumour evolution. *Nat Rev Genet 2020 224*. 2020;22(4):251-262.
358 doi:10.1038/s41576-020-00299-4
359 5. Landau DA, Clement K, Ziller MJ, et al. Locally Disordered Methylation Forms the
360 Basis of Intratumor Methylome Variation in Chronic Lymphocytic Leukemia. *Cancer*
361 *Cell*. 2014;26(6):813-825. doi:10.1016/j.ccell.2014.10.012
362 6. Pan H, Jiang Y, Boi M, et al. Epigenomic evolution in diffuse large B-cell lymphomas.
363 *Nat Commun*. 2015;6. doi:10.1038/ncomms7921
364 7. TCGA. Genomic and Epigenomic Landscapes of Adult De Novo Acute Myeloid
365 Leukemia. *N Engl J Med*. 2013;368(22):2059-2074. doi:10.1056/nejmoa1301689
366 8. Dawson MA, Prinjha RK, Dittman A, et al. Inhibition of BET recruitment to
367 chromatin as an effective treatment for MLL-fusion leukaemia. *Nature*.
368 2011;478(7370):529. doi:10.1038/NATURE10509
369 9. KM B, N Z, AU S, et al. MLL-rearranged leukemia is dependent on aberrant H3K79
370 methylation by DOT1L. *Cancer Cell*. 2011;20(1):66-78.
371 doi:10.1016/J.CCR.2011.06.010
372 10. Shlush LI, Zandi S, Mitchell A, et al. Identification of pre-leukaemic haematopoietic
373 stem cells in acute leukaemia. *Nature*. 2014;506(7488):328-333.
374 doi:10.1038/nature13038
375 11. Corces-Zimmerman MR, Hong WJ, Weissman IL, Medeiros BC, Majeti R.
376 Preleukemic mutations in human acute myeloid leukemia affect epigenetic regulators
377 and persist in remission. *Proc Natl Acad Sci U S A*. 2014;111(7):2548-2553.
378 doi:10.1073/pnas.1324297111
379 12. Domingues AF, Kulkarni R, Giotopoulos G, et al. Loss of KAT2A enhances
380 transcriptional noise and depletes acute myeloid leukemia stem-like cells. *Elife*.
381 2020;9. doi:10.7554/eLife.51754
382 13. Tzelepis K, Koike-Yusa H, De Braekeleer E, et al. A CRISPR Dropout Screen
383 Identifies Genetic Vulnerabilities and Therapeutic Targets in Acute Myeloid
384 Leukemia. *Cell Rep*. 2016;17(4):1193-1205. doi:10.1016/j.celrep.2016.09.079
385 14. Moris N, Edri S, Seyres D, et al. Histone Acetyltransferase KAT2A Stabilizes
386 Pluripotency with Control of Transcriptional Heterogeneity. *Stem Cells*.
387 2018;36(12):1828-1838. doi:10.1002/stem.2919
388 15. Somervaille TCP, Cleary ML. Identification and characterization of leukemia stem
389 cells in murine MLL-AF9 acute myeloid leukemia. *Cancer Cell*. 2006;10(4):257-268.

390 doi:10.1016/j.ccr.2006.08.020
391 16. Papaemmanuil E, Gerstung M, Bullinger L, et al. Genomic Classification and
392 Prognosis in Acute Myeloid Leukemia. *N Engl J Med*. 2016;374(23):2209.
393 doi:10.1056/NEJMOA1516192
394 17. Basheer F, Giotopoulos G, Meduri E, et al. Contrasting requirements during disease
395 evolution identify EZH2 as a therapeutic target in AML. *J Exp Med*. 2019;216(4):966-
396 981. doi:10.1084/jem.20181276
397 18. Ptasinska A, Assi SA, Mannari D, et al. Depletion of RUNX1/ETO in t(8;21) AML
398 cells leads to genome-wide changes in chromatin structure and transcription factor
399 binding. *Leukemia*. 2012;26(8):1829-1841. doi:10.1038/leu.2012.49
400 19. Mohammed H, Hernando-Herraez I, Savino A, Nichols J, Marioni JC, Correspondence
401 WR. Single-Cell Landscape of Transcriptional Heterogeneity and Cell Fate Decisions
402 during Mouse Early Gastrulation. *CellReports*. 2017;20:1215-1228.
403 doi:10.1016/j.celrep.2017.07.009
404 20. Cai X, Gao L, Teng L, et al. Runx1 Deficiency Decreases Ribosome Biogenesis and
405 Confers Stress Resistance to Hematopoietic Stem and Progenitor Cells. *Cell Stem Cell*.
406 2015;17(2):165-177. doi:10.1016/j.stem.2015.06.002
407 21. Trapnell C, Cacchiarelli D, Grimsby J, et al. The dynamics and regulators of cell fate
408 decisions are revealed by pseudotemporal ordering of single cells. *Nat Biotechnol*.
409 2014;32(4):381-386. doi:10.1038/nbt.2859
410 22. WC S, B R, AP W, et al. A conditional knockout resource for the genome-wide study
411 of mouse gene function. *Nature*. 2011;474(7351):337-344.
412 doi:10.1038/NATURE10163
413 23. Rodríguez CI, Buchholz F, Galloway J, et al. High-efficiency deleter mice show that
414 FLPe is an alternative to Cre-loxP. *Nat Genet 2000 252*. 2000;25(2):139-140.
415 doi:10.1038/75973
416 24. Dovey OM, Cooper JL, Mupo A, et al. Molecular synergy underlies the co-occurrence
417 patterns and phenotype of NPM1-mutant acute myeloid leukemia. *Blood*.
418 2017;130(17):1911-1922. doi:10.1182/BLOOD-2017-01-760595
419 25. Basheer F, Giotopoulos G, Meduri E, et al. Contrasting requirements during disease
420 evolution identify EZH2 as a therapeutic target in AML. *J Exp Med*. 2019;216(4):966-
421 981. doi:10.1084/jem.20181276
422